Limnol. Oceanogr., 58(1), 2013, 388–398

doi:10.4319/lo.2013.58.1.0388

The responses of eight coral reef calcifiers to increasing partial pressure of CO_2 do not exhibit a tipping point

S. Comeau,* P. J. Edmunds, N. B. Spindel, and R. C. Carpenter

Department of Biology, California State University, Northridge, California

Abstract

The objective of this study was to investigate whether a tipping point exists in the calcification responses of coral reef calcifiers to CO_2. We compared the effects of six partial pressures of CO_2 (P_{CO_2}) from 28 Pa to 210 Pa on the net calcification of four corals (*Acropora pulchra, Porites rus, Pocillopora damicornis,* and *Pavona cactus*), and four calcified algae (*Hydrolithon onkodes, Lithophyllum flavescens, Halimeda macroloba,* and *Halimeda minima*). After 2 weeks of acclimation in a common environment, organisms were incubated in 12 aquaria for 2 weeks at the targeted P_{CO_2} levels and net calcification was quantified. All eight species calcified at the highest P_{CO_2} in which the calcium carbonate aragonite saturation state was ~ 1. Calcification decreased linearly as a function of increasing partial P_{CO_2} in three corals and three algae. Overall, the decrease in net calcification as a function of decreasing pH was ~ 10% when ambient P_{CO_2} (39 Pa) was doubled. The calcification responses of *P. damicornis* and *H. macroloba* were unaffected by increasing P_{CO_2}. These results are inconsistent with the notion that coral reefs will be affected by rising P_{CO_2} in a response characterized by a tipping point. Instead, our findings combined among taxa suggest a gradual decline in calcification will occur, but this general response includes specific cases of complete resistance to rising P_{CO_2}. Together our results suggest that the overall response of coral reef communities to ocean acidification will be monotonic and inversely proportional to P_{CO_2}, with reef-wide responses dependent on the species composition of calcifying taxa.

Ocean acidification (OA), and its effects in synergy with rising temperature and a wide variety of local disturbances, is one of the major threats that coral reefs are facing in the next century (Erez et al. 2011). OA is caused by the dissolution of approximately one-quarter of anthropogenic CO_2 emissions into the ocean (Sabine et al. 2004), which induces a reaction with seawater promoting a series of chemical changes driving a decrease in pH, an increase in bicarbonate ion concentration [HCO_3^-], a decrease in carbonate ion concentration [CO_3^{2-}], and a lowered saturation state of calcium carbonate (Ω; Orr 2011).

The projected changes in carbonate chemistry of seawater are expected to threaten the long-term survival of tropical and cold-water scleractinians corals, and it has been proposed that coral reefs will cease to deposit calcium carbonate ($CaCO_3$) when the saturation state of aragonite (Ω_a, the mineral form of calcium carbonate used by corals) drops below 3.3 (Hoegh-Guldberg et al. 2007). It also has been proposed that coral reefs may exhibit a negative balance between precipitation and dissolution of $CaCO_3$ (i.e., they will lose more than they will deposit) when the concentration of atmospheric CO_2 relative to preindustrial levels doubles (Silverman et al. 2009). However, most studies of these effects are based on a limited set of empirical measurements establishing the functional relationship between the partial pressure of CO_2 (P_{CO_2}; and hence, Ω_{arag} and the saturation state of calcite, Ω_{calc}) and the calcification rates of important functional groups of calcifying taxa on tropical reefs (Erez et al. 2011; Edmunds et al. 2012). In addition, only one study (Marubini et al. 2008) to date has resolved precisely the shape of the relationship between calcification and P_{CO_2}, and therefore it is not possible to distinguish among functionally dissimilar relationships (Doney et al. 2009; Ries et al. 2009). The description of these relationships could greatly expand the understanding of the mechanisms of mineralization employed by calcifying organisms, and greatly improve the accuracy of models describing the effects of OA on calcifying organisms and ecosystems. Previous studies have suggested that a threshold P_{CO_2} (e.g., 50 Pa; Hoegh-Guldberg et al. 2007) exists, above which coral reef calcification will be dramatically reduced. For this reason, we investigated a large range of P_{CO_2} in order to test whether the existence of such critical thresholds can be demonstrated at an organismic level for eight of the main calcifiers in Moorea. When assessing the functioning of coral reefs in the future, the hypothesis that the calcification responses to P_{CO_2} of the main reef calcifiers exhibit tipping points must be critically evaluated. As has been shown at natural CO_2 vents in the marine environment, the crossing of a pH tipping point can lead to the abrupt disappearance of certain species (Hall-Spencer et al. 2008).

The effects of OA on calcification have been investigated in ≥ 21 species of scleractinian corals (Erez et al. 2011), and the results generally have demonstrated a decrease in calcification as a function of increasing P_{CO_2} and decreasing Ω_{arag} (Kleypas and Yates 2009; Erez et al. 2011). However, variation in experimental designs (such as the use of acid addition to simulate OA), or among-study differences in incubation conditions (such as light intensity, temperature, and the extent to which corals are fed), make generalizations about patterns of response difficult (Edmunds et al. 2012). The relationship between P_{CO_2} and calcification in reef organisms other than scleractinian corals has not been studied in detail, despite the important roles played by non-scleractinian organisms in reef ecosystem function. This is

* Corresponding author: steve.comeau@csun.edu

the case for crustose coralline algae (CCA) and articulated calcified algae, which are significant contributors to the $CaCO_3$ budget of coral reefs.

CCA play a critical role in the formation of coral reefs by cementing structural components together (Adey 1998) and providing settlement cues for coral larvae (Heyward and Negri 1999; Harrington et al. 2004). Because CCA produce skeletons made of high-magnesium calcite, the most soluble form of $CaCO_3$, they are expected to be particularly vulnerable to decreases in Ω_{calc} caused by OA (Anthony et al. 2008). The few published experimental studies on the response of CCA to OA tend to confirm this sensitivity, because decreased pH has negative effects on CCA through reduced recruitment (Hall-Spencer et al. 2008; Kuffner et al. 2008), depressed growth (Jokiel et al. 2008; Diaz-Pulido et al. 2012), lowered calcification rates (Anthony et al. 2008), and impaired capacity to induce coral larval settlement (Doropoulos et al. 2012). The articulated calcified alga *Halimeda* spp. serves as an important primary producer of organic and inorganic carbon on many coral reefs, and contributes to the diet of herbivorous fishes (Overholtzer and Motta 1999). In fact, *Halimeda* is the highest carbonate producer (64% of the total) among calcifying algae in the lagoon of Moorea French Polynesia (Payri 1988). *Halimeda* appears to respond to OA by linearly decreasing calcification as a function of decreasing pH (Sinutok et al. 2011) or as a curvilinear response to Ω_{arag} (Ries et al. 2009), although some studies have indicated a species-specific response (Price et al. 2011).

In light of the aforementioned studies, a global trend of the response of coral reef calcifiers to OA (Kleypas and Yates 2009) is emerging gradually, but progress toward this goal is slowed by a paucity of high-resolution descriptions of relationships between P_{CO_2} and calcification. These relationships are necessary to properly assess the threat to coral reefs from OA and to test the hypothesis that responses are characterized by 'tipping points' (Hansen et al. 2008). We performed experiments to establish a high-resolution relationship between P_{CO_2} and the calcification of four coral species, including two species with perforate skeletons (*Porites rus* and *Acropora pulchra*) and two species with imperforate skeletons (*Pocillopora damicornis* and *Pavona cactus*). In addition, the relationship between P_{CO_2} and calcification was quantified for four calcifying algae, including two CCA (*Hydrolithon onkodes* and *Lithophyllum flavescens*) with intracellular calcification and two articulated algal species (*Halimeda macroloba* and *H. minima*) that calcify extracellularly.

Methods

Experimental design and organism collection—This study was conducted from August to October 2011 in Moorea, French Polynesia, using organisms collected from the back reef of the north shore at ~ 1–2 m depth. Perturbation experiments were performed in a mesocosm apparatus consisting of 12 tanks that allowed for the maintenance of six P_{CO_2} treatments in duplicate. The experiment was separated into four consecutive trials, each lasting 2 weeks. The trials were used to create an independent contrast of the corals and algae by placing both taxa in the same tanks. In Trials 1 and 2, *P. rus* and *H. macroloba* were placed together in six tanks, and *A. pulchra* and *H. onkodes* were placed together in the six other tanks. In Trials 3 and 4, *P. damicornis* and *H. minima* were placed together in six tanks, with *P. cactus* and *L. flavescens* in the six other tanks. This procedure facilitated a statistical contrast among species of coral and among species of algae. It was not biologically meaningful to statistically compare corals and algae, so these groups were comingled in single tanks.

For each trial, 36 individual samples ('nubbins' for corals, 'cores' for CCA, and 'tufts' for *Halimeda*) of each species were collected, allowing for six replicates per species in each incubation tank. Samples of CCA were collected by coring (3.5–4.5 cm diameter), and coral nubbins (3–5 cm long branches) and *Halimeda* tufts (4–6 cm long thalli) were collected by hand. Freshly collected samples were returned to the Richard B. Gump South Pacific Research Station, where coral nubbins and CCA cores were glued with Z-Spar (A788 epoxy) to plastic bases (4 × 4 cm) and *Halimeda* tufts were attached to similar bases using nylon line.

Incubation conditions—After sample organisms were prepared as described above, they were maintained first for 2 d in a seawater table to recover from preparation. Afterward, they were transferred to a custom-made acclimation tank (Aqualogic) consisting of an open-flow (10 L min^{-1}) aquarium (1000 liters) in which temperature and light were adjusted to provide conditions similar to those used during the subsequent treatments (27°C, ~ 700 μmol photons m^{-2} s^{-1}). Four 75 W Light Emitting Diode (LED) modules (Sol White LED Module; Aqua-illumination) provided light to the acclimation tank on a 12 : 12 h light : dark cycle. Acclimation and treatments were performed at ~ 27°C (27.2° ± 0.02°C, mean ± SE, in the incubation tanks over the four trials) to match the annual mean temperature in the lagoon of Moorea. In the acclimation tank, organisms were submerged on a circular table that rotated once every 12 h to deliver a similar integrated light intensity over each day and remove effects associated with the position in the tank. Organisms remained in the acclimation tank for 2 weeks.

Seawater was supplied from a depth of 12 m in Cook's Bay, filtered through a sand filter (mesh size ~ 100 μm), and stored in a header tank from which it was gravity-fed to the acclimation tank and the mesocosms. After acclimation and for each trial, the 36 individuals from one species of coral and one species of algae were allocated randomly to six mesocosms (Aqualogic) of 150 liters at six different P_{CO_2} (for a final density of six coral nubbins and six algal pieces per tank), and individuals of the other coral and the other algal species were allocated randomly to the other six tanks experiencing identical conditions of P_{CO_2}, light, and temperature. During the mesocosm incubation of organisms from one trial (e.g., Trial 1), organisms for the following trial (e.g., Trial 2) were maintained in the acclimation tank so they could be placed into the mesocosm immediately following the preceding trial. Positions of organisms in all tanks

(including the acclimation tank) were changed randomly every 2 d to eliminate position effects. Seawater in the incubation tanks was replaced continuously at ~ 100 mL min^{-1}.

CO_2 treatments consisted of six P_{CO_2} levels corresponding to a preindustrial value (28 Pa), present-day concentration (39 Pa), an optimistic value expected by the end of the century (~ 55 Pa, approximate representative concentration pathway [RCP] scenario 4.5; Moss et al. 2010), an average value expected by the end of the century (~ 75 Pa, ~ RCP scenario 6.0), a pessimistic value expected by the end of the 21st century (~ 105 Pa, ~ RCP scenario 8.5), and an extreme value of 210 Pa. The extreme value was chosen to simulate seawater conditions at the saturation threshold with respect to aragonite ($\Omega_{arag} \sim 1$), the thermodynamic threshold between passive dissolution and precipitation of $CaCO_3$ in the aragonite crystal form. CO_2 treatments were obtained by bubbling the tanks with either CO_2-enriched air or CO_2-depleted air. CO_2-enriched air was created using a solenoid-controlled gas regulation system (Model A352, Qubit Systems) that mixed pure CO_2 with ambient air to create gas mixtures with a known P_{CO_2} (as detected by an Infrared Gas Analyzer, Model S151, Qubit Systems). CO_2-free air was obtained by scrubbing CO_2 from ambient air by passing it through a soda lime column. The flow of air and CO_2-manipulated air in each tank was adjusted independently using needle valves to correct the deviations detected by pH measurements of tank seawater from the targeted values.

Carbonate chemistry—Samples for seawater pH_T were collected 1–2 times d^{-1} (08:00 h and 18:00 h) in each tank, and measured immediately with an automatic titrator (T50, Mettler-Toledo) using a pH probe calibrated every third day on the total scale using 2-amino-2-hydroxymethyl-1,3-propanediol buffers (A. Dickson) at a salinity of 35.0. Calibrations were done every third day based on the rationale that the pH cell was demonstrably stable as it drifted an average of 0.2 mV between two calibrations, which corresponded to a pH_T variation of < 0.005 unit. The determination of pH using a pH cell was preferred over the use of the indicator dye m-cresol because the pH cell allowed for greater replication with only a trivial reduction in accuracy. Determination of pH using a pH cell yields uncertainty for pH measurements of < 0.02 unit for seawater (Dickson 2010). pH_T also was measured spectrophotometrically in each trial for every tank using the indicator dye m-cresol (Standard operating procedure 6b; Dickson et al. 2007). pH_T measured by the two methods provided similar values with a mean difference ≤ 0.008 pH units. Salinity was measured every 4 d using a conductivity meter (YSI 3100) and total alkalinity (A_T) was measured in duplicate every 2–3 d. Analyses of A_T were performed on the day of seawater sampling via an open-cell potentiometric titration using an automatic titrator (T50, Mettler-Toledo). Measurements of A_T were conducted on duplicate 50 mL samples at room temperature (~ 23°C), and A_T was calculated using a Gran function applied to pH values ranging from 3.5 to 3.0 as described by Dickson et al. (2007). Titrations of certified reference materials provided by A. G. Dickson (batch 105) yielded A_T values within 4.0 μmol kg^{-1} of the nominal value (SD = 4.1 μmol kg^{-1}; $n = 12$). Parameters of the carbonate system in seawater were calculated from salinity, temperature, A_T, and pH_T using the R package seacarb (Lavigne and Gattuso 2011).

Net calcification—Buoyant weight of the corals and algae (Spencer-Davies 1989) was recorded following 2 weeks of acclimation (i.e., before treatment incubation) and after 14 d of incubation in treatment conditions with a precision of ± 1 mg. The difference between the initial and final buoyant weight was converted to dry weight (dry wt) using an aragonite density of 2.93 g cm^{-3} for corals and *Halimeda,* and a calcite density of 2.71 g cm^{-3} for CCA. Rates of calcification were normalized to the area of the organisms, as estimated by the aluminum foil technique (Marsh 1970) for corals, and image analysis (Image J, U.S. National Institutes of Health) of planar digital images for CCA. For *Halimeda,* calcification was normalized to the final ash-free dry weight. To take into account the effects of P_{CO_2} on the tissue growth of corals, biomass also was estimated on all the specimens at the end of the incubation. To estimate biomass, corals were fixed in 10% formalin in seawater for 48 h and then decalcified in 5% HCl for 2–4 d. The tissue tunics left after skeletal dissolution were homogenized and then dried for 24–48 h at 60°C prior to weighing (± 1 mg). Biomass was used to standardize calcification rates and test for changes in the quantity of tissue per unit area induced by P_{CO_2}. For *P. cactus,* determination of biomass was impossible because their thin tissues were damaged during decalcification.

Statistical analysis—The assumptions of normality and equality of variance were evaluated through graphical analyses of residuals. All analyses were performed using R software (R Foundation for Statistical Computing). To test for a tank effect between Trials 1 and 2, as well as between Trials 3 and 4, P_{CO_2} treatments were analyzed using a 2-way model I ANOVA, with P_{CO_2} as a dependent variable, and Tank and Trial as a fixed effect.

Effects of each replicate trial on the response of calcification to the CO_2 treatments also were analyzed using a 2-way model I ANOVA, with calcification as a dependent variable, and CO_2 treatments and trials as fixed effects. When no significant effects of the Treatment × Trial interaction ($p \geq 0.25$; Quinn and Keough 2002) were detected, Trial was dropped from the analyses, and individual organisms treated as statistical replicates. To compare the response to OA of the different species studied, analyses of covariance (ANCOVA) were performed within each taxonomic group (corals, CCA, and *Halimeda*).

Model choice—An Akaike Information Criterion (AIC) approach was used to determine which model best described the relationship between calcification and P_{CO_2}. Three different models were tested: linear, logarithmic, and polynomial. These calculations were conducted for each organism studied using the software package R (R Foundation for Statistical Computing). The AIC for a given model (AIC_i) was calculated using

Table 1. Parameters of the carbonate chemistry of seawater in the 12 tanks, pooled among the four trials. The conditions are duplicates of the six targeted P_{CO_2} corresponding to a preindustrial value (28 Pa), a present day value (39 Pa), an optimistic value expected by the end of the century (~ 55 Pa, ~ RCP 4.5; Moss et al. 2010), an average value expected by the end of the century (~ 75 Pa, ~ RCP 6.0), a pessimistic value expected by the end of the 21st century (~ 105 Pa, ~ RCP 8.5), and an extreme value of 210 Pa. The concentration of dissolved inorganic carbon (C_T), partial pressure of CO_2 (P_{CO_2}), and the saturation state of aragonite (Ω_{arag}) and calcite (Ω_{calc}) were derived from pH_T, total alkalinity (A_T), salinity (S), and temperature (T) using the R package seacarb (Lavigne and Gattuso 2011). Values correspond to mean ± SE (n = 90; SE for the salinity was ~ 0).

Conditions	pH_T	A_T (μmol kg^{-1})	C_T (μmol kg^{-1})	P_{CO_2} (Pa)	Ω_{arag}	Ω_{calc}	T (°C)	S
28-1	8.184±0.005	2312±3	1871±5	26.5±0.4	4.58±0.02	6.89±0.06	27.2±0.04	36.4
28-2	8.188±0.006	2292±4	1868±5	26.2±0.5	4.61±0.03	6.94±0.06	27.3±0.06	36.4
39-1	8.035±0.004	2291±2	1989±4	41.1±0.4	3.61±0.04	5.44±0.04	27.2±0.05	36.3
39-2	8.052±0.004	2291±2	1961±4	38.9±0.4	3.68±0.04	5.55±0.04	27.3±0.05	36.3
55-1	7.938±0.005	2281±5	2018±5	53.7±0.8	3.00±0.03	4.51±0.04	27.2±0.06	36.3
55-2	7.946±0.005	2287±3	2018±4	52.6±0.8	3.05±0.03	4.59±0.04	27.3±0.04	36.2
75-1	7.817±0.006	2261±8	2061±8	74.2±1.4	2.37±0.03	3.57±0.04	27.2±0.07	36.3
75-2	7.809±0.006	2260±6	2064±6	75.8±1.4	2.33±0.03	3.51±0.04	27.2±0.04	36.3
105-1	7.703±0.008	2294±3	2143±4	102.1±2.2	1.94±0.03	2.91±0.05	27.1±0.03	36.1
105-2	7.701±0.008	2279±4	2130±5	101.8±2.0	1.91±0.03	2.88±0.04	27.2±0.06	36.2
210-1	7.418±0.008	2286±8	2243±8	208.7±3.7	1.07±0.02	1.61±0.03	27.2±0.02	36.3
210-2	7.407±0.007	2290±3	2251±4	214.1±3.4	1.05±0.02	1.57±0.03	27.3±0.05	36.4

$$\mathrm{AIC}_i = n \ln\left(\frac{\mathrm{RSS}}{n}\right) + 2k \quad (1)$$

where n is the number of data points, RSS is the residual sums of squares of the model, and k is the number of parameters in the model.

To quantify the plausibility of each model being the best approximation, the Akaike weights (W_i) then were calculated as

$$W_i = \frac{e^{(-0.5\Delta\mathrm{AIC}_i)}}{\sum_{R=1}^{R} e^{(-0.5\Delta\mathrm{AIC}_R)}} \quad (2)$$

where $\Delta\mathrm{AIC}_i$ is the difference between the AIC value for a given model and the minimum AIC value (the best fit) for the group of models investigated. The denominator is the sum of the relative likelihoods for the three models. The models with W_i that were within 10% of the maximum were not excluded from the study.

Results

There was no significant difference in P_{CO_2} between trials (ANOVA, between Trials 1 and 2: $F_{1,11} = 0.05$, $p = 0.827$; between Trials 3 and 4: $F_{1,11} = 0.46$, $p = 0.499$). The mean values for the carbonate chemistry parameters during the four trials were stable and centered on the targeted values (Table 1), and hence facilitated statistical comparisons between trials. The smallest variations between tanks for P_{CO_2} were obtained in the low-CO_2 treatment as well as the control; whereas, variation increased as P_{CO_2} increased. However, the variation in the high-P_{CO_2} treatment did not coincide with large variation in calcium carbonate saturation states (e.g., Ω_a SE = 0.02 at 210 Pa P_{CO_2}).

For net calcification, there were no significant effects of the Treatment × Trial interaction ($F_{5,60} < 1.3$, $p > 0.25$) for five species (*P. rus, A. pulchra, L. flavescens, H. macroloba,* and *H. minima*). The trial effect was significant for the remaining three species ($F_{5,60} = 1.869$, $p = 0.114$; $F_{5,60} = 4.753$, $p = 0.01$; and $F_{5,60} = 1.820$, $p = 0.123$ in *P. damicornis, P. cactus,* and *H. onkodes,* respectively), but a graphical analysis of the differences between trials in these cases demonstrated that the trial effect was due to a difference in magnitude and not direction of the treatment. For this reason, the trial effect also was dropped from the analysis for the eight species and the individual organisms treated as statistical replicates in the following analyses.

Net calcification of corals—The mean net calcification of corals over the 2 week incubations was positive in all six treatments (Fig. 1). The highest rates of net area-normalized calcification were measured for *P. rus* and *A. pulchra* (1.53 mg cm^{-2} d^{-1} ± 0.07 mg cm^{-2} d^{-1} [mean ± SE, n = 12] at 28 Pa and 1.41 mg cm^{-2} d^{-1} ± 0.08 mg cm^{-2} d^{-1} at 39 Pa P_{CO_2}, respectively). Maximum mean rates of area-normalized calcification were lower for *P. damicornis* and *P. cactus* (0.69 mg cm^{-2} d^{-1} ± 0.08 mg cm^{-2} d^{-1} at 55 Pa and 0.91 mg cm^{-2} d^{-1} ± 0.06 mg cm^{-2} d^{-1} at 55 Pa P_{CO_2}, respectively). The lowest area-normalized net calcification rates were recorded at 210 Pa P_{CO_2}, where they were 1.10 mg cm^{-2} d^{-1} ± 0.11 mg cm^{-2} d^{-1} in *P. rus,* 0.73 mg cm^{-2} d^{-1} ± 0.09 mg cm^{-2} d^{-1} in *A. pulchra,* 0.55 mg cm^{-2} d^{-1} ± 0.06 mg cm^{-2} d^{-1} in *P. damicornis,* and 0.58 mg cm^{-2} d^{-1} ± 0.05 mg cm^{-2} d^{-1} in *A. pulchra*. In the four coral species, area-normalized calcification declined linearly as a function of increasing P_{CO_2}. AIC results (Table 2) justified the use of linear regressions to describe the relationship between P_{CO_2} treatments and area-normalized calcification for the four coral species. The response of calcification to increasing P_{CO_2} was relatively similar in *P. rus, A. pulchra,* and *P. cactus,* with the strongest P_{CO_2}-dependent decline measured for *P. rus* and *A. pulchra* (with respective slopes of −21 and −31 μg cm^{-2} d^{-1} per 10 Pa of P_{CO_2} increase; Table 3). *P. cactus* was affected slightly less than *P. rus* and *A. pulchra,* with a linear regression slope of −19 μg cm^{-2} d^{-1} per 10 Pa of P_{CO_2}. There was no significant decline in area-normalized net calcification rate as a function of P_{CO_2} for *P. damicornis* (slope = −6 μg cm^{-2} d^{-1} per 10 Pa

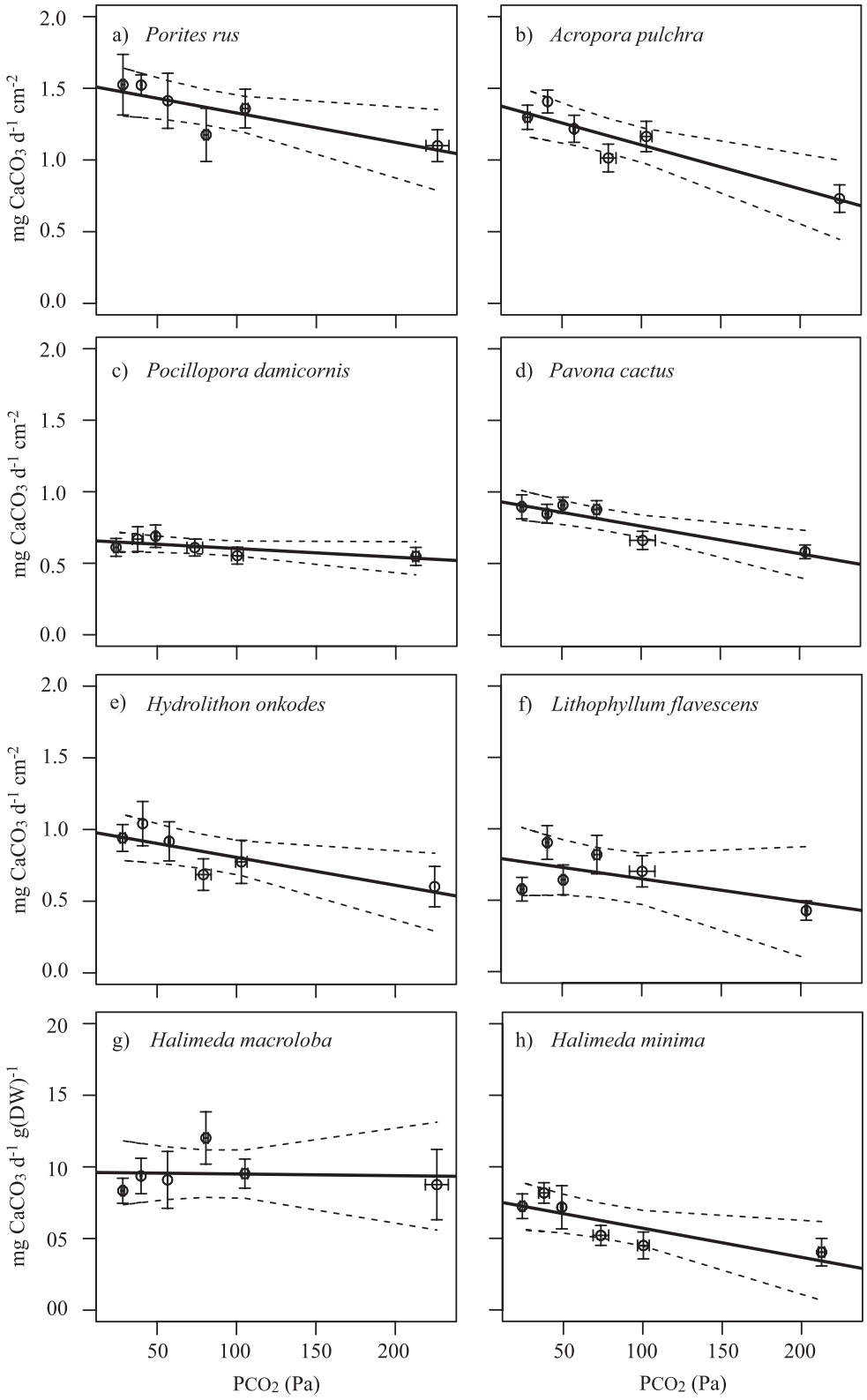

Fig. 1. Mean calcification as a function of P_{CO_2} in the eight species studied: (a) *P. rus,* (b) *A. pulchra,* (c) *P. damicornis,* (d) *P. cactus,* (e) *H. onkodes*, (f) *L. flavescens,* (g) *H. macroloba,* and (h) *H. minima*. The points correspond to the mean calcification, pooled between trials (n = 12), the vertical error bars show the SE of the measurements of calcification, and the horizontal error bars show the SE of P_{CO_2}. The dashed lines represent the 95% CIs of the linear regressions.

Table 2. Summary of the Akaike Information Criterion (AIC) used to determine the best model type (linear vs. logarithmic vs. polynomial) describing the relationship between calcification and P_{CO_2}. AIC_i is the AIC value for a given model, ΔAIC_i is the difference between the AIC value for a given model and the minimum AIC value (the best fitting) for the group of models investigated, and W_i is the Akaike weight. In the species column, the normalization parameter of calcification is given in parentheses.

Species	Model	AIC_i	ΔAIC_i	W_i
Porites rus (Area)	linear	120.0	0.43	0.38
	logarithmic	119.6	0.00	0.47
	polynomial	121.8	2.14	0.16
Acropora pulchra (Area)	linear	46.3	0.00	0.47
	logarithmic	47.0	0.69	0.33
	polynomial	48.0	1.69	0.20
Pavona cactus (Area)	linear	−8.8	0.00	0.52
	logarithmic	−7.3	1.45	0.25
	polynomial	−7.0	1.71	0.22
Pocillopora damicornis (Area)	linear	−0.8	0.00	0.44
	logarithmic	−0.5	0.25	0.39
	polynomial	1.1	1.91	0.17
Porites rus (Biomass)	linear	−145.2	4.91	0.04
	logarithmic	−150.1	0.00	0.49
	polynomial	−149.9	0.13	0.46
Acropora pulchra (Biomass)	linear	−61.7	6.36	0.03
	logarithmic	−66.4	1.69	0.29
	polynomial	−68.1	0.00	0.68
Pocillopora damicornis (Biomass)	linear	−193.9	0.44	0.33
	logarithmic	−194.3	0.00	0.41
	polynomial	−193.4	0.92	0.26
Hydrolithon onkodes (Area)	linear	94.5	0.71	0.33
	logarithmic	93.8	0.00	0.47
	polynomial	95.5	1.63	0.21
Lithophyllum flavescens (Area)	linear	60.0	1.03	0.34
	logarithmic	61.4	3.45	0.10
	polynomial	58.0	0.00	0.56
Halimeda macroloba (Ash-free dry weight)	linear	453.2	0.11	0.38
	logarithmic	453.1	0.00	0.41
	polynomial	454.4	1.31	0.21
Halimeda minima (Ash-free dry weight)	linear	290.4	2.28	0.15
	logarithmic	288.1	0.00	0.45
	polynomial	288.3	0.24	0.40

of P_{CO_2}, $p = 0.105$; Table 3). ANCOVA (Table 4) revealed that the intercepts of the relationships between calcification rate and P_{CO_2} differed significantly between the coral species studied, which demonstrated that they calcified at different rates. However, ANCOVA did not reveal differences in the slopes of the relationships between calcification rate and P_{CO_2}, although a strong trend was measured for *A. pulchra* and *P. damicornis* (Table 4; $p = 0.073$).

For biomass measured at the end of each incubation, as well as biomass-normalized calcification, AIC results (Table 2) confirmed the suitability of a non-linear polynomial function to describe the biomass-normalized calcification rate, and confirmed the relationship between biomass and area in *P. rus* and *A. pulchra* (Fig. 2; Table 3). In contrast, a linear model best described biomass-normalized calcification rate and biomass–area relationships in *P. damicornis.* For *P. rus* and *A. pulchra,* biomass increased with P_{CO_2} until reaching a maximum at ~ 150 Pa. Thereafter, it declined as P_{CO_2} approached 210 Pa (Fig. 2). For *P. damicornis,* biomass slightly decreased linearly as a function of increasing P_{CO_2} (Fig. 2). These changes in biomass due to P_{CO_2} in both *P. rus* and *A. pulchra* resulted in a decrease in biomass-normalized calcification (~ 9–10% per 10 Pa of P_{CO_2}) until P_{CO_2} reached ~ 80–100 Pa, where it remained relatively constant as P_{CO_2} approached 210 Pa. Because biomass declined slightly as a function of increasing P_{CO_2}, while area-normalized calcification slightly increased, the biomass-normalized net calcification rate in *P. damicornis* was unaffected by P_{CO_2}.

Net calcification of algae—Similar to the responses of the corals, the four species of calcifying algae also exhibited positive mean net calcification over the 2 week incubations in all treatments (Fig. 1), and the relationships between P_{CO_2} treatments and calcification were best described using linear regressions (Table 2). Both CCA exhibited a significant decrease in net calcification as a function of increasing P_{CO_2} (Table 3). Calcification in CCA was depressed by ~ 0.1 mg cm^{-2} d^{-1} and 0.3 mg cm^{-2} d^{-1} in *H. onkodes* and *L. flavescens,* respectively, at 28 Pa compared with ambient P_{CO_2} (~ 39 Pa). The lowest calcification rates (but not significantly different from the 105 Pa treatment) were measured in both species at 210 Pa (0.60 mg cm^{-2} d^{-1} ± 0.14 mg cm^{-2} d^{-1} and

Table 3. Parameters of the linear and non-linear regressions used to estimate the relationship between calcification and P_{CO_2}. Linear regressions were used to represent the relationship between area-normalized calcification and P_{CO_2} for the four corals and the two CCA, and for the relationship between biomass-normalized calcification and P_{CO_2} for the two *Halimeda* species and the coral *P. damicornis.* The relationship between biomass-normalized calcification and P_{CO_2} was best fit by a polynomial function ($y = ax^2 + bx + c$) for *P. rus* and *A. pulchra. P*-values of the slopes, as well as R^2 for the linear regressions, are given; *p*-values for the intercepts of the linear regressions were < 0.001. The *p*-values given for the non-linear regressions correspond to the constants a, b, c in the model $y = ax^2 + bx + c$.

Normalization	Species	Values	*p*	R^2
Area	*Porites rus*	$-2.10\ 10^{-4}x+1.54$	0.038	0.70
	Acropora pulchra	$-3.07\ 10^{-4}x+1.41$	0.010	0.84
	Pocillopora damicornis	$-6.05\ 10^{-5}x+0.66$	0.105	0.52
	Pavona cactus	$-1.92\ 10^{-4}x+0.95$	0.013	0.82
Biomass	*Porites rus*	$7.42\ 10^{-8}x^2-2.58\ 10^{-4}x+0.29$	0.083, 0.044, 0.004	0.89
	Acropora pulchra	$1.40\ 10^{-7}x^2-4.47\ 10^{-4}x+0.51$	0.111, 0.076, 0.007	0.78
	Pocillopora damicornis	$3.58\ 10^{-6}x+0.12$	0.75	0.04
Area	*Hydrolithon onkodes*	$-1.94\ 10^{-4}x+1.00$	0.040	0.69
	Lithophyllum flavescens	$-1.60\ 10^{-4}x+0.81$	0.044	0.37
Biomass	*Halimeda macroloba*	$-1.17\ 10^{-4}x+9.62$	0.902	0.00
	Halimeda minima	$-2.03\ 10^{-3}x+7.74$	0.042	0.69

0.43 mg cm^{-2} d^{-1} ± 0.07 mg cm^{-2} d^{-1} in *H. onkodes* and *L. flavescens*, respectively). Results from the ANCOVA showed that the intercepts of the calcification–CO_2 relationships for the two CCA were significantly different ($p = 0.024$) but the slopes were not ($p = 0.681$; Table 5), which indicated that elevated P_{CO_2} affected both species in a similar manner.

For *Halimeda,* the two species displayed contrasting responses to P_{CO_2}. For *H. macroloba,* calcification was unaffected by P_{CO_2}, but for *H. minima,* it decreased linearly with increasing P_{CO_2} (Table 3), with a minimum at 210 Pa P_{CO_2} (4.03 mg $CaCO_3$ d^{-1} g[dry wt]$^{-1}$). The results of the ANCOVA confirmed the different biomass-normalized calcification–CO_2 relationships for the two *Halimeda* by revealing a significant difference between species for intercepts ($p < 0.001$) as well as slopes ($p = 0.046$; Table 5).

Discussion

Effects of OA on corals—The response of corals to OA is species-dependent (Edmunds et al. 2012). The two species with perforate skeletons (*P. rus* and *A. pulchra*) exhibited similar responses in calcification to P_{CO_2}; whereas, the two corals with imperforate skeletons responded differently from one another, with *P. damicornis* being less sensitive to increasing P_{CO_2} than *P. cactus* (Fig. 3a). Erez et al. (2011) reviewed the effects of OA on corals and demonstrated that a doubling of P_{CO_2} induced highly variable responses in calcification that ranged from no effect to a ~ 100% reduction in net calcification; most of the studies reviewed reported results that fell within a range of 15–50% decline in net calcification. The responses in calcification observed in our study were below this range. The strongest effect of increasing P_{CO_2} was measured for *A. pulchra* and *P. cactus* (9% decline in area-normalized calcification at 78 Pa vs. 39 Pa) and the weakest effect on *P. damicornis* (4% decline in area-normalized calcification at 78 Pa vs. 39 Pa; Fig. 3). The present study is not the first to show a relatively small effect of OA on corals, with null results following increasing P_{CO_2} reported for the temperate coral *Cladocora caespitosa* (Rodolfo-Metalpa et al. 2010) and the tropical coral *Stylophora pistillata* at ambient temperatures (Reynaud et al. 2003) and fed massive *Porites* spp. at 25.6°C and 29.3°C (Edmunds 2011).

In our study, biomass-normalized calcification did not show a similar trend to area-normalized calcification in response to P_{CO_2}. Whereas area-normalized calcification decreased linearly with P_{CO_2} in *P. rus* and *A. pulchra,*

Table 4. Results of the ANCOVA used to test for differences in slopes and intercepts in the relationships between area-normalized calcification and P_{CO_2} in the four coral species tested by pair.

Species 1	Species 2	Effect	Residuals df	SS	*F*	*p*
P. rus	*A. pulchra*	intercept	69	0.805	4.971	0.029
		slope	68	0.001	0.007	0.935
	P. cactus	intercept	69	8.398	49.530	<0.001
		slope	68	0.001	0.005	0.944
	P. damicornis	intercept	69	13.246	76.626	<0.001
		slope	68	0.208	1.202	0.277
A. pulchra	*P. cactus*	intercept	69	1.707	21.787	<0.001
		slope	68	0.009	0.113	0.738
	P. damicornis	intercept	69	4.196	51.382	<0.001
		slope	68	0.271	3.314	0.073
P. cactus	*P. damicornis*	intercept	69	0.614	11.538	0.001
		slope	68	0.037	0.703	0.405

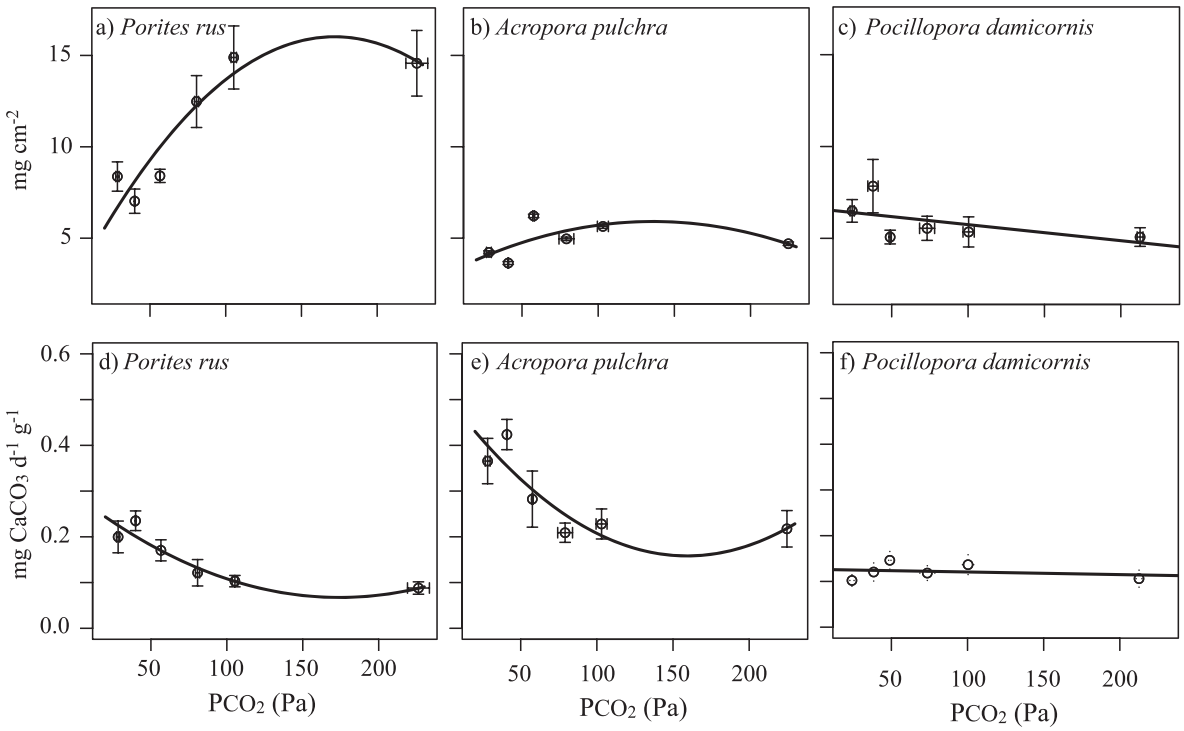

Fig. 2. Biomass and biomass-normalized calcification in three corals. (a–c) is biomass (mg cm^{-2}) for (a) *P. rus,* (b) *A. pulchra,* and (c) *P. damicornis.* (d–f) is the biomass-normalized calcification for (d) *P. rus,* (e) *A. pulchra,* and (f) *P. damicornis.* The points correspond to the mean after pooling the two trials ($n = 12$), the vertical error bars show the SE of the measurements of biomass or calcification, and the horizontal error bars show the SE of P_{CO_2}.

biomass-normalized calcification followed a similar change relative to the control treatment explained best by a polynomial model for both species (Fig. 3b). This result was due to a corresponding increase in biomass as a function of increasing P_{CO_2}, with a maximum at ~ 150 Pa, which was ~ 2.5-fold and 2-fold greater than samples in the control treatment in *P. rus* and *A. pulchra,* respectively (Fig. 2). This result is in agreement with Edmunds (2011), who showed an increase in biomass in massive *Porites* spp. at 81.5 Pa compared with 38.4 Pa at 29.3°C. For both *P. rus* and *A. pulchra,* we propose that increasing P_{CO_2}, and, hence, increasing [HCO_3^-], may favor photosynthetic efficiency of *Symbiodinium,* leading to an increase in the production of organic carbon that can be stored in coral tissues. When P_{CO_2} reached ~ 150 Pa for *P. rus* and *A. pulchra,* we suspect that the *Symbiodinium* may have been saturated with HCO_3^- and perhaps were realizing the negative effects of low pH in disrupting cellular function such as enzymatic activity (Pörtner et al. 2004). In contrast, for *P. damicornis,* biomass slightly decreased as a linear function of increasing P_{CO_2} (~ 5% when ambient P_{CO_2} doubled). In this species, the cost of maintaining relatively high calcification rates (i.e., no effect of P_{CO_2} on area-normalized calcification) at high P_{CO_2} may not have been compensated by an increase in *Symbiodinium* photosynthesis, and therefore biomass declined as it was metabolized as a respiratory substrate.

Effects of OA on calcifying algae—In the two species of CCA, calcification decreased as a function of increasing P_{CO_2}, as observed for *A. pulchra* and *P. cactus* (for which calcification declined 8% when P_{CO_2} doubled from the ambient condition). More adverse effects of OA on CCA have been reported by Anthony et al. (2008) and Diaz-Pulido et al. (2012), who both observed net dissolution as well as loss of net production in *H. onkodes* exposed to ~ 100 Pa P_{CO_2}. The reported dissolution in these studies might be due to exposure of the underside of the calcified

Table 5. Results of the ANCOVA used to test for differences in slopes and intercepts in the relationships between area-normalized calcification and P_{CO_2} for the two CCA (*H. onkodes* and *L. flavescens*) and between biomass-normalized calcification and P_{CO_2} for the two *Halimeda* (*H. macroloba* and *H. minima*).

Species 1	Species 2	Effect	Residuals df	SS	*F*	*p*
H. onkodes	*L. flavescens*	intercept	69	0.885	5.181	0.024
		slope	68	0.029	0.169	0.681
H. macroloba	*H. minima*	intercept	69	367.4	17.034	<0.001
		slope	68	87.3	4.045	0.046

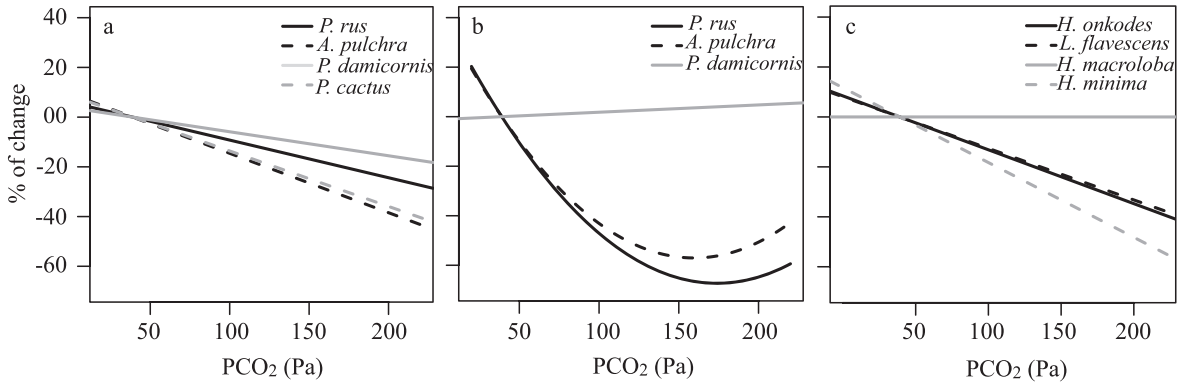

Fig. 3. Compilation of the relationships between P_{CO_2} and calcification. The values correspond to the percent of change in calcification relative to present day P_{CO_2} (~ 39 Pa). (a) Percent change in area-normalized calcification in the four coral species; (b) percent change in biomass-normalized calcification in *P. rus, A. pulchra,* and *P. damicornis;* and (c) percent change in calcification of the four algae studied.

thallus that lacks living tissue, which might otherwise provide protection against micro-eroders (Chazottes et al. 1995) and dissolution that can occur in seawater supersaturated with respect to calcium carbonate (Kline et al. 2012). In the present study, the lower surface of the CCA was covered with epoxy resin to more closely simulate the natural configuration of the algae on natural surfaces of the reef where seawater does not have direct access to the lower carbonate surface of the thallus.

The response to OA by *H. minima* was similar to that of CCA exposed to increasing P_{CO_2} (calcification in *H. minima* declined by ~ 11% when ambient P_{CO_2} doubled), whereas P_{CO_2} did not affect *H. macroloba* (Fig. 3). Contrasting relationships between P_{CO_2} and calcification in *Halimeda* have been reported, including a curvilinear response (Ries et al. 2009), a strong decline in calcification and even dissolution (with P_{CO_2} at ~ 200 Pa; Sinutok et al. 2011), or species-specific responses (Price et al. 2011). The differences in light levels (i.e., the light level used by Sinutok et al. (2011) is only 43% that employed in the present study), the degree of water motion, and species composition between studies likely are to be the causes of such differences. Furthermore, calcification in *Halimeda,* which takes place within intercellular spaces within the thallus (Borowitzka and Larkum 1987), is likely to be linked strongly to photosynthesis and respiration, and thus dependent on the species-specific responses of these physiological processes to OA. In contrast, in CCA, calcification takes place within the cell wall (Borowitzka and Larkum 1987) and appears to be more directly linked to seawater carbonate chemistry, as shown by the similar reduction in calcification in both CCA species in this study.

Effects of OA on the reef community—In contrast to previous studies that have predicted rapid decreases in calcification of corals and coral reefs exposed to $P_{CO_2} >$ 50 Pa (Hoegh-Guldberg et al. 2007; Silverman et al. 2009), our study, performed at the organismic level on eight of the main calcifiers in Moorea, suggests that tropical reefs might not be affected by OA as strongly or as rapidly as previously supposed (Pandolfi et al. 2011). Importantly, we found an overall decrease in calcification of only ≤ 11% with a doubling of P_{CO_2}. Furthermore, when P_{CO_2} was increased to 210 Pa (double the pessimistic value expected by the end of the century; Moss et al. 2010), we did not detect a threshold at which the effect of P_{CO_2} on calcification became nonlinear and intensified (i.e., a tipping point). It is likely that both biological and methodological effects can explain the reason that the effects of OA on calcification are more limited in the present study compared with previous work (reviewed in Erez et al. 2011). Our experiments were carried out at the end of the Austral winter, when corals typically have high food reserves (Thornhill et al. 2011), and therefore might contain more reserves of energy that could be used to counteract the deleterious effects of low pH. Second, we used an acclimation tank to reduce the effects of collection stress (Tentori and Allemand 2006), and minimize variance attributed to unique microenvironments from which the organisms were collected. The pre-incubation acclimation period also allowed the organisms to acclimate to experimental conditions (i.e., temperature, light, and water quality) that were not part of the experimental manipulation (involving P_{CO_2}). Finally, we provided light intensities during the incubations that were ecologically relevant (700 μmol photons m^{-2} s^{-1}) compared with the light intensities used in many recent studies of related topics (i.e., 11.5–600 μmol photons m^{-2} s^{-1}; Edmunds et al. 2012), and therefore our analyses are ecologically relevant to shallow tropical reefs.

Tropical reefs in the central South Pacific might not be the first coral reefs in the world to be affected as OA intensifies in the next century, because the seawater saturation states for $CaCO_3$ in this region are relatively high (Ω_{arag} = 3.7–4.2; S. Comeau, unpubl.; Alldredge 2012) and are expected to remain largely supersaturated with respect to both aragonite and calcite through the end of the current century (Ω_{arag} = 2.4–2.7, which corresponds to the 75 Pa treatment in our study [A_T ~ 2350 μmol kg^{-1}; 27°C]). The variety of responses to high P_{CO_2} reported here and elsewhere (Erez et al. 2011) demonstrate a broad and consistent theme of heterogeneity in the response of reef calcifiers to OA (Pandolfi et al. 2011; Edmunds et al. 2012) and the emergence of potential 'ecological winners,' such as *P. damicornis* and *H. macroloba,* at least based on

resistance to high P_{CO_2}. Such resistance to decreasing pH potentially may be due to the capacity to up-regulate pH at the site of calcification (McCulloch et al. 2012), which might be a critical factor in determining the dominant species in the high-CO_2 oceans of the future. The study of natural CO_2 vents in Papua New Guinea have confirmed that some taxa, such as massive *Porites* spp., can become dominant at high P_{CO_2} values that mimic future OA conditions (Fabricius et al. 2011). The lack of a clear tipping point, as well as the emergence of potential winners in the face of declining pH, indicate that in the coming decades the species composition of coral reefs is likely to slowly change, without abrupt transitions, to a new composition in which species able to tightly control pH at their calcification site will outcompete species unable to maintain such control.

Acknowledgments

We thank H. Rouzé and A. Spindel for field and laboratory assistance; the U.S. National Science Foundation for financial support; Division of Ocean Science (OCE) 10-41270; and the Moorea Coral Reef Long Term Ecological Research site (OCE 04-17413 and 10-26852); as well as the Gordon and Betty Moore Foundation for logistic support. Thanks are also due to the two anonymous reviewers for useful comments on an earlier version of this paper. This is contribution 188 of the California State University, Northridge, Marine Biology Program.

References

Adey, W. H. 1998. Coral reefs: Algal structured and mediated ecosystems in shallow, turbulent, alkaline waters. J. Phycol. **34:** 393–406, doi:10.1046/j.1529-8817.1998.340393.x

Alldredge, A. 2012. MCR LTER: Coral reef: Water column: Offshore ocean acidification: Water profiles, CTD, and chemistry. Internet [accessed 2012 Aug 04], available from http://metacat.lternet.edu/knb/metacat/knb-lter-mcr.1037.1/lter.

Anthony, K. R. N., D. I. Kline, G. Diaz-Pulido, S. Dove, and O. Hoegh-Guldberg. 2008. Ocean acidification causes bleaching and productivity loss in coral reef builders. Proc. Natl. Acad. Sci. **105:** 17442–17446, doi:10.1073/pnas.0804478105

Borowitzka, M. A., and A. W. D. Larkum. 1987. Calcification in algae: Mechanisms and the role of metabolism. Crit. Rev. Plant Sci. **6:** 1–45, doi:10.1080/07352688709382246

Chazottes, V., T. L. Campion-Alsumard, and M. Peyrot-Clausade. 1995. Bioerosion rates on coral reefs: Interactions between macroborers, microborers and grazers (Moorea, French Polynesia). Palaeogeogr. Palaeoclimatol. Palaeoecol. **113:** 189–198, doi:10.1016/0031-0182(95)00043-L

Diaz-Pulido, G., K. R. N. Anthony, D. I. Kline, S. Dove, and O. Hoegh-Guldberg. 2012. Interactions between ocean acidification and warming on the mortality and dissolution of coralline algae. J. Phycol. **48:** 32–39, doi:10.1111/j.1529-8817.2011.01084.x

Dickson, A. G. 2010. The carbon dioxide system in seawater: equilibrium chemistry and measurements, p. 17–40. *In* U. Riebesell, V. J. Fabry, L. Hansson, and J.-P. Gattuso [eds.], Guide to best practices for ocean acidification research and data reporting. Publications Office of the European Union. Online at http://www.epoca-project.eu/index.php/guide-to-best-practices-for-ocean-acidification-research-and-data-reporting.html

———, C. L. Sabine, and J. R. Christian [eds.]. 2007.Guide to best practices for ocean CO_2 measurements. PICES Special Publication 3.

Doney, S. C., V. J. Fabry, R. A. Feely, and J. A. Kleypas. 2009. Ocean acidification: The other CO_2 problem. Annu. Rev. Mar. Sci. **1:** 169–192, doi:10.1146/annurev.marine.010908.163834

Doropoulos, C., S. Ward, G. Diaz-Pulido, O. Hoegh-Guldberg, and P. J. Mumby. 2012. Ocean acidification reduces coral recruitment by disrupting intimate larval-algal settlement interactions. Ecol. Lett. **4:** 338–346, doi:10.1111/j.1461-0248.2012.01743.x

Edmunds, P. J. 2011. Zooplanktivory ameliorates the effects of ocean acidification on the reef coral *Porites* spp. Limnol. Oceanogr. **56:** 2402–2410, doi:10.4319/lo.2011.56.6.2402

———, D. Brown, and V. Moriarty. 2012. Interactive effects of ocean acidification and temperature on two scleractinian corals from Moorea, French Polynesia. Glob. Change Biol. **18:** 2173–2183, doi:10.1111/j.1365-2486.2012.02695.x

Erez, J., S. Reynaud, J. Silverman, K. Schneider, and D. Allemand. 2011. Coral calcification under ocean acidification and global change, p. 151–176. *In* Z. Dubinsky and N. Stambler [eds.], Coral reefs: An ecosystem in transition. Springer.

Fabricius, K. E., and others. 2011. Losers and winners in coral reefs acclimatized to elevated carbon dioxide concentrations. Nat. Clim. Change **1:** 165–169, doi:10.1038/nclimate1122

Hall-Spencer, J. M., R. Rodolfo-Metalpa, S. Martin, E. Ransome, M. Fine, S. M. Turner, S. J. Rowley, D. Tedesco, and M.-C. Buia. 2008. Volcanic carbon dioxide vents show ecosystem effects of ocean acidification. Nature **454:** 96–99, doi:10.1038/nature07051

Hansen, J., and others. 2008. Target atmospheric CO_2: Where should humanity aim? Open Atmos. Sci. J. **2:** 217–231.

Harrington, L., K. Fabricius, G. De'ath, and A. Negri. 2004. Recognition and selection of settlement substrata determine post-settlement survival in corals. Ecology **85:** 3428–3437, doi:10.1890/04-0298

Heyward, A. J., and A. Negri. 1999. Natural inducers for coral larval metamorphosis. Coral Reefs **18:** 273–279, doi:10.1007/s003380050193

Hoegh-Guldberg, O., and others. 2007. Coral reefs under rapid climate change and ocean acidification. Science **318:** 1737–1742, doi:10.1126/science.1152509

Jokiel, P. L., K. S. Rodgers, I. B. Kuffner, A. J. Andersson, E. F. Cox, and F. T. MacKenzie. 2008. Ocean acidification and calcifying reef organisms: A mesocosm investigation. Coral Reefs **27:** 473–483, doi:10.1007/s00338-008-0380-9

Kleypas, J., and K. Yates. 2009. Coral reefs and ocean acidification. Oceanography **22:** 108–117, doi:10.5670/oceanog.2009.101

Kline, D. I., and others. 2012. A short-term in situ CO_2 enrichment experiment on Heron Island (GBR). Sci. Rep. **2:** 413, doi:10.1038/srep00413

Kuffner, I. B., A. J. Andersson, P. L. Jokiel, K. S. Rodgers, and E. T. Mackenzie. 2008. Decreased abundance of crustose coralline algae due to ocean acidification. Nat. Geosci. **1:** 114–117, doi:10.1038/ngeo100

Lavigne, H., and J.-P. Gattuso. 2011. seacarb: Seawater carbonate chemistry with R. R package version 2.4.1 [accessed on 2012 Jun 01]. Available from http://CRAN.Rproject.org/package=seacarb

Marubini, F., C. Ferrier-Pagès, P. Furla, and D. Allemand. 2008. Coral calcification responds to seawater acidification: A working hypothesis towards a physiological mechanism. Coral Reefs **27:** 491–499, doi:10.1007/s00338-008-0375-6

Marsh, J. A. 1970. Primary productivity of reef-building calcareous red algae. Ecology **51:** 255–263, doi:10.2307/1933661

McCulloch, M., J. Falter, J. Trotter, and P. Montagna. 2012. Coral resilience to ocean acidification and global warming through pH up-regulation. Nat. Clim. Change **2:** 623–627, doi:10.1038/nclimate1473

Moss, R. H., and others. 2010. The next generation of scenarios for climate change research and assessment. Nature **463:** 747–756, doi:10.1038/nature08823

Orr, J. C. 2011. Recent and future changes in ocean carbonate chemistry, p. 41–66. *In* J.-P. Gattuso and L. Hansson [eds.], Ocean acidification. Oxford Univ. Press.

Overholtzer, K., and P. Motta. 1999. Comparative resource use by juvenile parrotfishes in the Florida Keys. Mar. Ecol. Prog. Ser. **177:** 177–187, doi:10.3354/meps177177

Pandolfi, J. M., S. R. Connolly, D. J. Marshall, and A. L. Cohen. 2011. Projecting coral reef futures under global warming and ocean acidification. Science **333:** 418–422, doi:10.1126/science.1204794

Payri, C. E. 1988. *Halimeda* contribution to organic and inorganic production in a Tahitian reef system. Coral Reefs **6:** 251–262, doi:10.1007/BF00302021

Pörtner, H. O., M. Langenbuch, and A. Reipschläger. 2004. Biological impact of elevated ocean CO_2 concentrations: Lessons from animal physiology and earth history. J. Oceanogr. **60:** 705–718, doi:10.1007/s10872-004-5763-0

Price, N. N., S. L. Hamilton, J. S. Tootell, and J. E. Smith. 2011. Species-specific consequences of ocean acidification for the calcareous tropical green algae *Halimeda*. Mar. Ecol. Prog. Ser. **440:** 67–68, doi:10.3354/meps09309

Quinn, G. P., and M. J. Keough. 2002. Experimental design and data analysis for biologists. Cambridge Univ. Press.

Reynaud, S., N. Leclercq, S. Romaine-Lioud, C. Ferrier-Pagès, J. Jaubert, and J.-P. Gattuso. 2003. Interacting effects of CO_2 partial pressure and temperature on photosynthesis and calcification in a scleractinian coral. Glob. Change Biol. **9:** 1660–1668, doi:10.1046/j.1365-2486.2003.00678.x

Ries, J. B., A. L. Cohen, and D. C. McCorkle. 2009. Marine calcifiers exhibit mixed responses to CO_2-induced ocean acidification. Geology **37:** 1131–1134, doi:10.1130/G30210A.1

Rodolfo-Metalpa, R., S. Martin, C. Ferrier-Pagès, and J.-P. Gattuso. 2010. Response of the temperate coral *Cladocora caespitosa* to mid- and long-term exposure to P_{CO_2} and temperature levels projected for the year 2100. Biogeosciences **7:** 289–300, doi:10.5194/bg-7-289-2010

Sabine, C. L., and others. 2004. The oceanic sink for anthropogenic CO_2. Science **305:** 367–371, doi:10.1126/science.1097403

Silverman, J., B. Lazar, L. Cao, K. Caldeira, and J. Erez. 2009. Coral reefs may start dissolving when atmospheric CO_2 doubles. Geophys. Res. Lett. **36:** L05606, doi:10.1029/2008GL036282

Sinutok, S., R. Hill, M. A. Doblin, R. Wuhrer, and P. J. Ralph. 2011. Warmer more acidic conditions cause decreased productivity and calcification in subtropical coral reef sediment-dwelling calcifiers. Limnol. Oceanogr. **56:** 1200–1212, doi:10.4319/lo.2011.56.4.1200

Spencer-Davies, P. 1989. Short-term growth measurements of corals using an accurate buoyant weighing technique. Mar. Biol. **101:** 389–95, doi:10.1007/BF00428135

Tentori, E., and D. Allemand. 2006. Light-enhanced calcification and dark decalcification in isolates of the soft coral *Cladiella* sp. during tissue recovery. Biol. Bull. **211:** 193–202, doi:10.2307/4134593

Thornhill, D. J., and others. 2011. A connection between colony biomass and death in Caribbean reef-building corals. PLoS One **6:** e29535, doi:10.1371/journal.pone.0029535

Associate editor: Anthony W. D. Larkum

Received: 26 June 2012
Accepted: 06 November 2012
Amended: 06 November 2012